# A systematic study of the superdeformation of Pb isotopes with relativistic mean field theory*

GUO Jian-You(郭建友)[1;1)] SHENG Zong-Qiang(圣宗强)[2] FANG Xiang-Zheng(方向正)[1]

1 (School of Physics and Material Science, Anhui University, Hefei 230039, China)
2 (Department of Mathematics and Physics, Anhui University of Science and Technology, Huainan 232001, China)

**Abstract** The microscopically constrained relativistic mean field theory is used to investigate the superdeformation for Pb isotopes. The calculations have been performed with the four different interactions NL3, PK1, TM1 and NLSH, and show that there exists a clear superdeformed minimum in the potential energy surfaces. The excitation energy, deformation and depth of the well in the superdeformed minimum are comparable for the four different interactions. Furthermore the trend for the change of the superdeformed excitation energy with neutron number is correctly reproduced. The calculated two-neutron separation energy in the ground state and superdeformed minimum together with their differences are in agreement with the available data. The larger energy difference appearing in the superdeformed minimum reflects a lower average level density at superdeformations for Pb isotopes.

**Key words** Pb isotopes, superdeformation, relativistic mean field theory

**PACS** 21.10.-k, 21.60.Jz, 21.10.Dr

## 1 Introduction

Superdeformation (SD) of atomic nuclei is one of the most interesting topics of nuclear structure studies. Over the past two decades, many rotational bands associated with SD shapes have been observed in several regions of the nuclear chart[1], with 85 SD bands observed in nuclei with $79 < Z < 84$ (the $A \sim 190$ region) alone, where impressive knowledge on SD bands has been obtained. Unfortunately, despite the rather large amount of experimental information on SD bands, there are still a number of very interesting properties, which have not yet been measured. The characteristic physical observables are the spin, parity and excitation energy relative to the ground state of the SD bands. The difficulty lies in the observation of the very weak discrete transitions linking the SD levels with levels of normal deformation (ND levels). Until now, the transitions linking SD and ND levels have been observed only in a few nuclei in the $A \sim 190$ region: two bands in $^{194}$Hg[2, 3], and one band in each of $^{194}$Pb[4, 5], $^{192}$Pb[6], and $^{191}$Hg[7]. Less precise measurements have been achieved in $^{192}$Hg[8] and $^{195}$Pb[9], following the analysis of the quasi-continuum component of the decay. Recently, the measurement of the excitation energy of the yrast (lowest energy for a given spin) SD band in $^{196}$Pb has been reported[10]. Together with earlier measurements of the excitation energies of SD states in $^{194}$Pb and $^{192}$Pb, this allows a systematic study of the energy of the SD well in a single isotopic chain. Many theoretical models have been employed to study these superdeformed states of atomic nuclei. The Strutinsky method with a Woods-Saxon potential[11], the Hartree-Fock-Bogoliubov method with different mean field parameterizations[12—14], and the cluster model[15] have provided predictions on the excitation energy of SD bands, where a gross trend of decreasing energy with decreasing neutron number is obtained for the Pb isotopes. However, the absolute energies as well as their differences are not consistently reproduced by these models as the analysis in Ref. [10] shows. Given that the relativistic mean field (RMF) theory[16] has gained considerable success in describ-

Received 26 February 2008

* Supported by National Natural Science Foundation of China (10475001, 10675001), Program for New Century Excellent Talents in University of China (NCET-05-0558), Program for Excellent Talents in Anhui Province University (2007Z018), and Education Committee Foundation of Anhui Province (2006KJ259B)

1) E-mail: jianyou@ahu.edu.cn

ing many nuclear phenomena for stable nuclei[17, 18] as well as nuclei even far from stability[19], as discussed in great detail in the recent review articles[20, 21] and in the references given therein, it has also been applied to estimate the excitation energies and well depths for the SD bands. The data of the SD minima of $^{194}$Hg and $^{194}$Pb have been predicted in considerable agreement with experiment[22]. Here we will report on a systematic investigation of the SD states for the Pb isotopes by a microscopic, self-consistent quadrupole deformation constrained relativistic mean field theory with pairing treated by the BCS method. Our results show perfect manifestation of the SD structure in Pb isotopes including the evolution of the excitation energy, well depth, deformation and shell structure. Also the ND states are well reproduced.

## 2 Theory

The starting point of the RMF theory is a standard Lagrangian density where the nucleons are described as Dirac particles which interact via the exchange of various mesons including the isoscalar-scalar $\sigma$ meson, the isoscalar-vector $\omega$ meson and the isovector-vector $\rho$ meson. The effective Lagrangian density considered is written in the form:

$$\begin{aligned}\mathcal{L} = {} & \bar{\psi}_i\left(\mathrm{i}\not{\partial}-M\right)\psi_i+\frac{1}{2}\partial_\mu\sigma\partial^\mu\sigma-U(\sigma)-g_\sigma\bar{\psi}_i\sigma\psi_i- \\ & \frac{1}{4}\Omega_{\mu\nu}\Omega^{\mu\nu}+\frac{1}{2}m_\omega^2\omega_\mu\omega^\mu-g_\omega\bar{\psi}_i\not{\omega}\psi_i- \\ & \frac{1}{4}\boldsymbol{R}_{\mu\nu}\boldsymbol{R}^{\mu\nu}+\frac{1}{2}m_\rho^2\boldsymbol{\rho}_\mu\boldsymbol{\rho}^\mu-g_\rho\bar{\psi}_i\not{\boldsymbol{\rho}}\boldsymbol{\tau}\psi_i- \\ & \frac{1}{4}F_{\mu\nu}F^{\mu\nu}-e\bar{\psi}_i\frac{1-\tau_3}{2}\not{\boldsymbol{A}}\psi_i, \end{aligned} \tag{1}$$

where $\bar{\psi}=\psi^\dagger\gamma^0$ and $\psi$ is the Dirac spinor. $M$ is the nucleon mass and $m_\sigma(g_\sigma)$, $m_\omega$ $(g_\omega)$, and $m_\rho$ $(g_\rho)$ are the masses (coupling constants) of the respective mesons. $U(\sigma)=\frac{1}{2}m_\sigma^2\sigma^2+\frac{1}{3}g_2\sigma^3+\frac{1}{4}g_3\sigma^4$ is a nonlinear scalar self-interaction of $\sigma$ mesons. The field tensors for the vector mesons are represented as $\Omega^{\mu\nu}=\partial^\mu\omega^\nu-\partial^\nu\omega^\mu$, $\boldsymbol{R}^{\mu\nu}=\partial^\mu\boldsymbol{\rho}^\nu-\partial^\nu\boldsymbol{\rho}^\mu-g^\rho(\boldsymbol{\rho}^\mu\times\boldsymbol{\rho}^\nu)$, and $F^{\mu\nu}=\partial^\mu\boldsymbol{A}^\nu-\partial^\nu\boldsymbol{A}^\mu$.

The Dirac equation for the nucleons and the Klein-Gordon type equations for the mesons and the photon are given by a variational principle and can be solved by expanding the wavefunctions in terms of the eigenfunctions of a deformed axially symmetric harmonic-oscillator potential[23] or a Woods-Saxon potential[24]. The details can be found in Ref. [18] and references therein.

The potential energy curve can be calculated microscopically within the constrained RMF theory. The binding energy at certain deformation value is obtained by constraining the quadruple moment $\langle Q_2\rangle$ to a given value $\mu_2$ in the expectation value of the Hamiltonian[25],

$$\langle H'\rangle=\langle H\rangle+\frac{1}{2}C_\mu\left(\langle Q_2\rangle-\mu_2\right)^2, \tag{2}$$

where $C_\mu$ is the corresponding Lagrangian multiplier.

For the nuclei studied in this paper a deformed harmonic oscillator basis has been used, leading to a very good convergence of the numerical calculation of the binding energy and deformation. The converged deformations corresponding to different $\mu_2$'s are not sensitive to the deformation parameter $\beta_0$ of the harmonic oscillator basis in a reasonable range if the basis is taken large enough. The different choices of $\beta_0$ lead to different iteration numbers of the self-consistent calculation and different computation time. Physical quantities such as the binding energy and the deformation change very little. Thus the deformation parameter $\beta_0$ of the harmonic oscillator basis is chosen near the expected deformation to obtain high accuracy and low computation time. By varying $\mu_2$, the binding energies at different deformations can be obtained. The pairing is treated in the constant gap approximation (BCS), in which the pairing gap is taken as $12/\sqrt{A}$ for an even number of nucleons.

## 3 Numerical results

The four interactions NL3[26], PK1[27], TM1[28] and NLSH[29] listed in Table 1 are adopted to investigate the properties of superdeformed states. The potential energy curves obtained for $^{190-204}$Pb are shown in the Figs. 1, 2, 3, and 4, respectively, where the energy of the ground state has been taken as a reference. $E_x$ and $V$ are the excitation energy and depth of the well of the SD minimum as shown in the subfigure for $^{196}$Pb in Fig. 1. Similar patterns are found for all the effective interactions. Most of the

Table 1. The parameter sets of interactions NL3, PK1, TM1 and NLSH with the masses in the units of MeV.

| | $M_{\rm n}$ | $M_{\rm p}$ | $M_\sigma$ | $M_\omega$ | $M_\rho$ | $g_\sigma$ | $g_\omega$ | $g_\rho$ | $g_2$ | $g_3$ | $c_3$ |
|---|---|---|---|---|---|---|---|---|---|---|---|
| NL3 | 939 | 939 | 508.1941 | 782.501 | 763 | 10.2169 | 12.8675 | 4.4744 | −10.4307 | −28.8851 | 0 |
| PK1 | 939.5731 | 938.2796 | 514.0891 | 784.254 | 763 | 10.3222 | 13.0131 | 4.5297 | −8.1688 | −9.9976 | 55.636 |
| TM1 | 938 | 938 | 511.198 | 783 | 770 | 10.0289 | 12.6139 | 4.6322 | −7.2325 | 0.6183 | 71.3075 |
| NLSH | 939 | 939 | 526.05921 | 783 | 763 | 10.44355 | 12.9451 | 4.38281 | −6.90992 | −15.83373 | 0 |

curves exhibit a clear SD minimum for the Pb isotopes, especially for the nuclei with higher neutron number. For $^{190,192}$Pb, the calculated SD minimum is not very pronounced, it even disappears for the interaction NLSH. For $^{190}$Pb, the RMF theory predicts a considerably higher excitation energy and shallower well in the SD minimum in comparison with its neighboring nucleus $^{192}$Pb, which implies that it is difficult to form a stable SD state. For $^{192}$Pb, although having a shallower well, it has a relatively low excitation energy, which indicates that it is relatively easy to form the SD state as observed in experiment. Starting from $^{194}$Pb, the RMF theory predicts that the excitation energy increases with increasing neutron number together with an increase of the well depth. So, the SD states can still be formed in these nuclei, which agrees with the experimental observations. However for the $N > 118$ nuclei the excitation energy is very high which makes it difficult to excite the SD states. This may explain why in the Pb isotopic chain one observes the SD nuclear states only for neutron numbers between $N = 110$ and $N = 116$. Besides the success in describing SD states, the RMF theory predicts also a well known interesting feature of the ground state deformation, i.e. the evolution of the shape from prolate to oblate before, and finally to spherical shapes just when reaching the neutron shell closure at $N = 126$. From Figs. 1—4, on can see that the ground state of $^{190}$Pb exhibits a coexistence between the prolate and oblate shape with about a 5 MeV stiff barrier between them. With increasing neutron number, the ground state of the Pb isotopes gradually moves towards the oblate side with smaller and smaller deformation. Finally a fully spherical $^{204}$Pb can be seen.

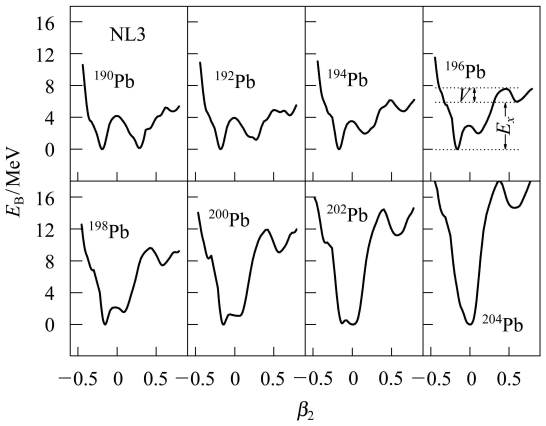


Fig. 1. The potential energy curves for $^{190—204}$Pb obtained by the constrained RMF theory with the interactions NL3, where the $E_x$ and $V$ represent respectively for the excitation energy relative to the ground state of superdeformed minimum and the depth of well of superdeformed minimum. The ground state binding energy is taken as a reference.

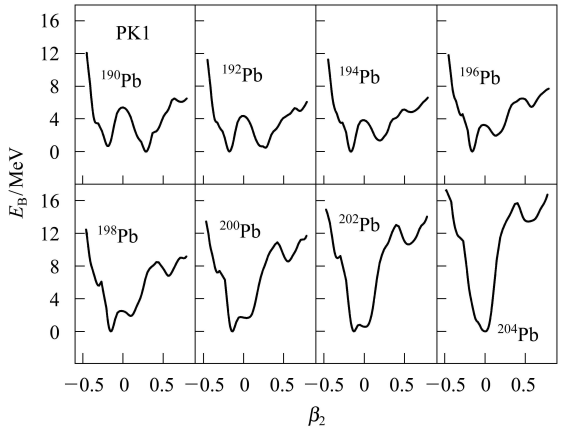


Fig. 2. The same as Fig. 1, but with PK1.

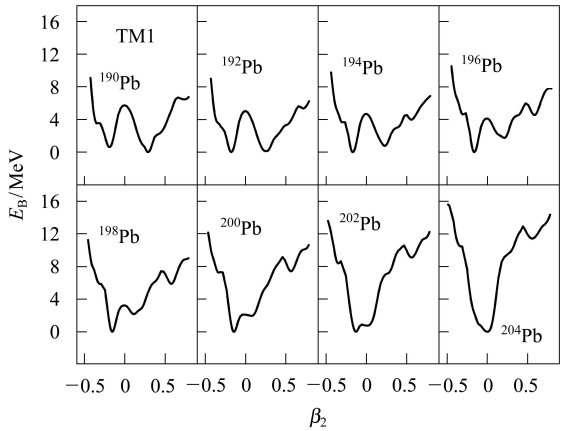


Fig. 3. The same as Fig. 1, but with TM1.

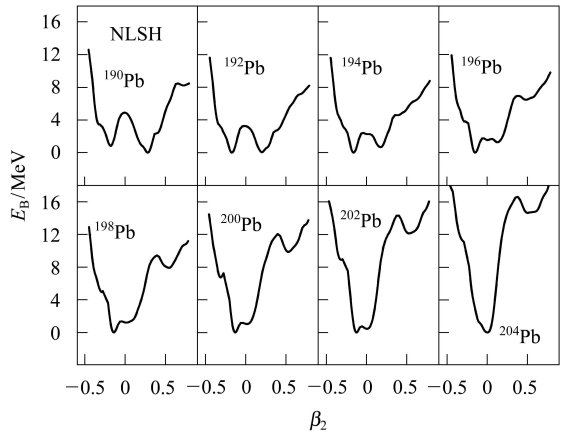


Fig. 4. The same as Fig. 1, but with NLSH.

The bandhead energies of the SD bands for Pb isotopes are listed in Table 2. It can be seen that for the NL3 interactions, the calculated excitation energies are in excellent agreement with the available data. The maximum deviation between theory and experiment is less than 0.34 MeV. For the PK1 interactions, except for a marginal overestimation of the excitation energy for $^{192}$Pb, the theoretical prediction

Table 2. The SD bandhead energies of Pb isotopes $E_x$ as a function of the neutron number obtained by the constrained RMF calculations with the interactions NL3, PK1, TM1 and NLSH, in comparison with data available.

| Pb isotopes | $E_x$/MeV | | | | |
|---|---|---|---|---|---|
| | NL3 | PK1 | TM1 | NLSH | EXP |
| $^{190}$Pb | 4.761 | 6.076 | 6.454 | | |
| $^{192}$Pb | 4.259 | 4.966 | 5.348 | | 4.011 |
| $^{194}$Pb | 4.764 | 4.838 | 3.960 | | 4.643 |
| $^{196}$Pb | 5.969 | 5.458 | 4.558 | 6.478 | 5.630 |
| $^{198}$Pb | 7.421 | 6.817 | 5.863 | 7.926 | |
| $^{200}$Pb | 9.061 | 8.565 | 7.407 | 9.876 | |
| $^{202}$Pb | 11.195 | 10.644 | 9.091 | 12.137 | |
| $^{204}$Pb | 14.649 | 13.447 | 11.417 | 14.640 | |

is highly consistent with the experiment. With the TM1 interaction the excitation energy is overestimated for $^{192}$Pb and underestimated for $^{194,196}$Pb. Using the NLSH interaction, the RMF theory fails to reproduce the SD minimum for $^{192,194}$Pb. Although there are some deviations between the theoretical calculation and the data, the trend of the change of the excitation energy with neutron number is correctly reproduced with all effective interactions, which can be seen in Fig. 5. The interaction TM1 shows the least agreement with the experimental data, as can be seen from Fig. 5. Starting from $^{194}$Pb the excitation energy lies below the experimental data and the results calculated with the other interactions. Comparing the four interactions, NL3 is definitely superior to all the other ones in describing the SD states, despite the fact that the more recently developed interaction PK1 gives a similar good description of the ground states of the Pb isotopes with mass numbers below 200 (see Table 3 and Fig. 5 in Ref. [27]). In contrast to the RMF calculations, the Strutinsky method with a Woods-Saxon potential[11], the Hartree-Fock-Bogoliubov method with different mean field parameterizations[12—14] and the cluster model[15] predict only the gross trend of decreasing energy with decreasing neutron number. The absolute energies and their differences are not consistently reproduced by these models. The RMF theory gives a much better description of the SD excitation energies of the Pb isotopes.

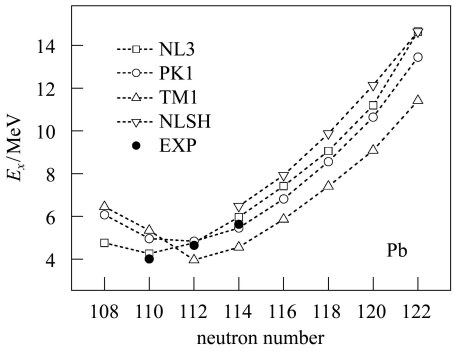


Fig. 5. The SD bandhead energies of Pb isotopes $E_x$ as a function of the neutron number obtained by the constrained RMF calculations with the interactions NL3 (□), PK1 (○), TM1 (△) and NLSH (▽) in comparison with the experimental data[10] (●).

Besides the excitation energy, the deformation and well depth of the SD minimum are two other important parameters characterizing the properties of the superdeformed states. In particular, the well depth affects the life time of the superdeformed states. In Table 3, the quadruple deformations $\beta_2$ and the depths of the superdeformed minima $V$ in the superdeformed states for $^{190—204}$Pb are listed in the upper and lower panels, respectively. Except for a few cases, the deformation of the SD minima lies systematically in the range between 0.5 and 0.7 for all the four different interactions NL3, PK1, TM1 and NLSH. This agrees with the observation that superdeformed nuclei adopt ellipsoidal shapes with an axis ratio around 2:1[1]. The RMF theory predicts a barrier height lower than 1 MeV for $^{190,192}$Pb and higher than 1 MeV for $^{196—214}$Pb for all the considered interactions. For $^{194}$Pb, the estimated barriers are considerable different for the various interactions.

Table 3. The quadruple deformation $\beta_2$ and the depth of the superdeformed minimum $V$ in the superdeformed states of $^{190—204}$Pb obtained by the constrained RMF theory with the interactions NL3, PK1, TM1 and NLSH.

| $\beta_2$ | NL3 | PK1 | TM1 | NLSH |
|---|---|---|---|---|
| $^{190}$Pb | 0.718 | 0.719 | 0.739 | |
| $^{192}$Pb | 0.700 | 0.699 | 0.718 | |
| $^{194}$Pb | 0.658 | 0.577 | 0.557 | |
| $^{196}$Pb | 0.600 | 0.578 | 0.579 | 0.478 |
| $^{198}$Pb | 0.580 | 0.561 | 0.578 | 0.539 |
| $^{200}$Pb | 0.562 | 0.558 | 0.561 | 0.538 |
| $^{202}$Pb | 0.562 | 0.541 | 0.560 | 0.521 |
| $^{204}$Pb | 0.562 | 0.541 | 0.559 | 0.502 |
| $V$/MeV | NL3 | PK1 | TM1 | NLSH |
| $^{190}$Pb | 0.464 | 0.422 | 0.229 | |
| $^{192}$Pb | 0.662 | 0.348 | 0.258 | |
| $^{194}$Pb | 1.380 | 0.296 | 0.599 | |
| $^{196}$Pb | 1.602 | 1.029 | 1.418 | 0.469 |
| $^{198}$Pb | 2.177 | 1.660 | 1.569 | 1.517 |
| $^{200}$Pb | 2.836 | 2.341 | 1.752 | 2.178 |
| $^{202}$Pb | 3.259 | 2.371 | 1.487 | 2.173 |
| $^{204}$Pb | 3.515 | 2.248 | 1.490 | 1.967 |

The two-neutron separation energy defined as $S_{2n}(Z,N) = E(Z,N) - E(Z,N-2)$ is a sensitive quantity to test a microscopic theory. Here $E(Z,N)$ is the binding energy of a nucleus with proton number $Z$ and neutron number $N$. In Table 4 the calculated two-neutron separation energies in the ground

state $S_{2n,\mathrm{ND}}$ and SD minimum $S_{2n,\mathrm{SD}}$ for the Pb isotopes are shown in comparison with the experimental data[10, 30]. It can be seen that the RMF calculations with all the four different interactions reproduce the experimental data for $S_{2n,\mathrm{ND}}$ quite well. The maximum deviation between the calculations and data is less than 1.7 MeV, especially for the NL3, the deviations are within 1 MeV. The calculated $S_{2n,\mathrm{SD}}$ are for all four interactions close to the available data. Both, the calculations and the experimental data show that $S_{2n,\mathrm{ND}}$ and $S_{2n,\mathrm{ND}}$ vary smoothly with the neutron number. No sharp drop in the binding energy is seen in the $S_{2n}$, which indicates that in the Pb isotope chain no significant shell gap appears in the ground state or SD state.

Table 4. Two-neutron separation energy in the ground state and superdeformation minimum obtained by the constrained RMF theory with the interactions NL3, PK1, TM1 and NLSH, in comparison with data available.

| $N$ | $S_{2n,\mathrm{ND}}$/MeV | | | | |
|---|---|---|---|---|---|
| | NL3 | PK1 | TM1 | NLSH | EXP |
| 110 | 17.862 | 16.915 | 16.716 | 17.984 | 18.400 |
| 112 | 17.537 | 17.207 | 17.135 | 17.444 | 17.810 |
| 114 | 17.173 | 16.885 | 16.636 | 17.255 | 17.320 |
| 116 | 16.739 | 16.440 | 16.124 | 16.899 | 16.820 |
| 118 | 16.287 | 16.050 | 15.595 | 16.652 | 16.295 |
| 120 | 15.709 | 15.241 | 14.886 | 15.150 | 15.837 |
| 122 | 16.360 | 15.287 | 14.927 | 15.611 | 15.318 |
| $N$ | $S_{2n,\mathrm{SD}}$/MeV | | | | |
| | NL3 | PK1 | TM1 | NLSH | |
| 110 | 18.364 | 18.025 | 17.908 | | |
| 112 | 17.031 | 17.334 | 18.436 | | 17.16(4) |
| 114 | 15.968 | 16.266 | 16.037 | | 16.31(4) |
| 116 | 15.287 | 15.081 | 14.820 | 15.499 | |
| 118 | 14.648 | 14.303 | 14.051 | 14.653 | |
| 120 | 13.574 | 13.161 | 13.202 | 13.361 | |
| 122 | 12.906 | 12.484 | 12.601 | 12.637 | |

In order to reveal further detailed information on the shell structure, the two-neutron separation energy differences $\Delta S_{2n}(Z,N) = S_{2n}(Z,N) - S_{2n}(Z,N+2)$ are presented in Table 5 together with the experimental data[10, 30]. Here $\Delta S_{2n,\mathrm{ND}}$ and $\Delta S_{2n,\mathrm{SD}}$ represent the corresponding quantities for the ground state and superdeformed minimum, respectively. Table 5 shows that the experimental $\Delta S_{2n,\mathrm{ND}}$ changes of typically around 0.5 MeV are, with some exceptions, well reproduced in the RMF calculations with all the interactions. Compared with the other interactions, NL3 gives a better agreement with the experiment. Only for $^{204}$Pb is the deviation relatively large. Furthermore, the calculated $\Delta S_{2n,\mathrm{ND}}$ show very little differences for the nuclei with neutron numbers between $N = 112$ and $N = 118$, consistent with the experimental data. This suggests that there is no shell closure at $N = 112$ or $N = 114$ as predicted by other calculations. Compared with the ND states, the SD separation energies $S_{2n}$ are significantly larger than the typical ND value of 0.5 MeV, possibly reflecting a lower average level density at superdeformations. In particular, the $\Delta S_{2n,\mathrm{SD}}$ are obviously rather different for different nuclei. The $\Delta S_{2n,\mathrm{SD}}$ for these nuclei with $N$=112, 114, 118 are much larger than those of their neighboring nuclei, suggesting a larger shell gap in the SD states of $^{112,114,118}$Pb.

Table 5. Two-neutron separation energy difference in the ground state and superdeformation minimum obtained by the constrained RMF theory with the interactions NL3, PK1, TM1 and NLSH, in comparison with data available.

| $N$ | $\Delta S_{2n,\mathrm{ND}}$/MeV | | | | |
|---|---|---|---|---|---|
| | NL3 | PK1 | TM1 | NLSH | EXP |
| 110 | 0.325 | −0.292 | −0.419 | 0.540 | 0.590 |
| 112 | 0.364 | 0.322 | 0.499 | 0.189 | 0.490 |
| 114 | 0.434 | 0.445 | 0.512 | 0.356 | 0.500 |
| 116 | 0.452 | 0.390 | 0.529 | 0.247 | 0.525 |
| 118 | 0.578 | 0.809 | 0.709 | 1.502 | 0.458 |
| 120 | −0.651 | −0.046 | −0.041 | −0.461 | 0.519 |
| $N$ | $\Delta S_{2n,\mathrm{SD}}$/MeV | | | | |
| | NL3 | PK1 | TM1 | NLSH | EXP |
| 110 | 1.333 | 0.691 | −0.528 | | |
| 112 | 1.063 | 1.068 | 2.399 | | 0.85(8) |
| 114 | 0.681 | 1.185 | 1.217 | | |
| 116 | 0.639 | 0.778 | 0.769 | 0.846 | |
| 118 | 1.074 | 1.142 | 0.849 | 1.292 | |
| 120 | 0.668 | 0.677 | 0.601 | 0.724 | |

In summary, the superdeformation in $^{190-204}$Pb has been investigated by the constrained RMF theory employing all the most commonly used interactions, i.e., NL3, PK1, TM1 and NLSH. The calculations show a clear SD minimum at nearly all the potential energy curves for the Pb isotopes with similar patterns for all the effective interactions. The trend of the change of the excitation energies with neutron number is correctly reproduced. The calculated deformation of the SD minima lies systemically between 0.5 and 0.7, and is consistent with the observations from experiments. The two-neutron separation energies in the ground state and the SD minimum are well reproduced, varying smoothly with the neutron number. Compared with the typical value of 0.5 MeV for the ND states, the SD separation energies $S_{2n}$ are significantly larger, possibly reflecting a lower average level density at superdeformation.

## References


1 Singh B, Zywina R, Firestone R B. Nuclear Data Sheets, 2002, **97**: 241
2 Khoo T L, Carpenter M P, Lauritsen T et al. Phys. Rev. Lett., 1996, **76**: 1583
3 Hackman G, Khoo T L, Carpenter M P et al. Phys. Rev. Lett., 1997, **79**: 4100
4 Lopez-Martens A, Hannachi F, Korichi A et al. Phys. Lett. B, 1996, **380**: 18
5 Hauschild K, Bernstein L A, Becker J A et al. Phys. Rev. C, 1997, **55**: 2819
6 Wilson A N, Dracoulis G D, Byrne A P et al. Phys. Rev. Lett., 2003, **90**: 142501
7 Siem S, Reiter P, Khoo T L et al. Phys. Rev. C, 2004, **70**: 014303
8 Lauritsen T, Khoo T L, Ahmad I et al. Phys. Rev. C, 2000, **62**: 044316
9 Johnson M S, Cizewski J A, Ding K Y et al. Phys. Rev. C, 2005, **71**: 044310
10 Wilson A N, Singh A K, Hübel H et al. Phys. Rev. Lett., 2005, **95**: 182501
11 Satula W et al. Nucl. Phys. A, 1991, **529**: 289
12 Krieger S J et al. Nucl. Phys. A, 1992, **542**: 43
13 Heenen P H, Dobaczewski J, Nazarewicz W et al. Phys. Rev. C, 1998, **57**: 1719
14 Libert J, Girod M, Delaroche J P. Phys. Rev. C, 1999, **60**: 054301
15 Adamian G G, Antonenko N V, Jolos R V et al. Phys. Rev. C, 2004, **69**: 054310
16 Serot B, Walecka J D. Adv. Nucl. Phys., 1996, **16**: 1
17 Reinhard P G. Rep. Prog. Phys., 1989, **52**: 439
18 Ring P. Prog. Part. Nucl. Phys., 1996, **37**: 193
19 MENG J. Nucl. Phys. A, 1998, **635**: 3
20 Afanasjevb A V, Lalazissisc G A, Ring P. Phys. Rep., 2005, **409**: 101
21 MENG J, Toki H, ZHOU S G, ZHANG S Q, LONG W H, GENG L S. Prog. Part. Nucl. Phys., 2006, **57**: 470
22 Lalazissis G A, Ring P. Phys. Lett. B, 1998, **427**: 225
23 Gambhir Y, Ring P. Thimet A. Ann. Phys. (N.Y.), 1990, **198**: 132
24 ZHOU S G, MENG J, Ring P. Phys. Rev. C, 2003, **68**: 034323
25 Ring P, Schuck P. The Nuclear Many Body Problem. Springer, 1980
26 Lalazissis G A, König J, Ring P. Phys. Rev. C, 1997, **55**: 540
27 LONG W H, MENG J, Giai N V, ZHOU S G. Phys. Rev. C, 2004, **69**: 034319
28 Sugahara Y, Toki H. Nucl. Phys. A, 1994, **579**: 557
29 Sharma M M, Nagarajan M A, Ring P. Phys. Lett. B, 1993, **312**: 377
30 Audi G, Wapstra A H. Nucl. Phys. A, 1995, **595**: 409